Hindawi
Journal of Chemistry
Volume 2018, Article ID 6207910, 12 pages
https://doi.org/10.1155/2018/6207910

Research Article

Synthesis of Zeolites Materials Using Fly Ash and Oil Shale Ash and Their Applications in Removing Heavy Metals from Aqueous Solutions

A. Hamadi and K. Nabih

Laboratory of Applied Solid State Chemistry, Department of Chemistry, Faculty of Science, Mohammed V University, B.P. 1014 Rabat, Morocco

Correspondence should be addressed to A. Hamadi; hamadi_13@yahoo.fr

Received 7 March 2018; Revised 12 September 2018; Accepted 18 September 2018; Published 23 October 2018

Academic Editor: Henryk Kozlowski

Fly ash and oil shale ash generated from power plants can be transformed to suitable materials usable for removal of heavy metals. Due to their high silica content, fly ash and oil shale ash have been considered as the main stone of zeolite synthesis. In this work, we synthesized zeolites from class F fly ash (FA) and modified oil shale ash (MOSA) by alkaline fusion followed by refluxing. Our synthesis process focused on the effect of quantity of NaOH on the crystallinity of the reaction products: Na-P1 and Na-P2 type zeolites synthesized, respectively, from FA and MOSA. The effect of NaOH mass (1, 2, 4, and 8 g) was investigated with the following synthesis conditions: 2 h fusion at 650°C, 2 h agitation, and refluxing for 12 hours. The experimental results demonstrated that the crystallinity of Na-p1 and Na-P2 zeolites increased with increasing the mass of NaOH. The resulting products were characterized with X-ray diffraction, FTIR, and scanning electron microscopy. The reaction products ZV4 and ZM4 synthesized, respectively, from FA and MOSA and containing main zeolite phases with a crystallinity of 92.7% of Na-P1 and 83.6% of Na-P2, respectively, were chosen as adsorbents for the adsorption experiments. Series of experiments were carried out to study the removal of lead, zinc, and chromium by ZV4 and ZM4. The results allowed us to know the optimal conditions of adsorption for the three heavy metals. Adsorption data have been interpreted in terms of Langmuir and Freundlich isotherms. The results showed that lead has a higher affinity for ZM4 than ZV4 and zinc has similar adsorption efficiency for both sorbents that was remarkably reduced for chromium. The results of the present work suggest that zeolites synthesized from MOSA may be considered as effective as those synthesized from FA for heavy metals adsorption.

1. Introduction

Heavy metals are widespread in nature under many forms. Small concentrations of these elements have been demonstrated to be essential for human health, but in high levels, they can be harmful and may cause serious damage to central nervous system, lungs, kidneys, and liver. As heavy metals solubility increases when pH decreases, various treatment techniques have been proposed for their removal from aqueous solutions including chemical precipitation, membrane filtration, electrolytic processes (reverse osmosis and electrodialysis), solvent extraction, and adsorption [1–5]. Unfortunately, most of these techniques have been reported to be expensive and have many inconveniences like low selectivity, high energy requirement, and generation of other harmful waste. However, adsorption is believed to be an effective technique due to its high selectivity, and it can also ensure better environmental conditions.

As reported by the World Bank, the world currently produces about 4 billion tons of all types of waste per year [6]. Affecting seriously human health and ecological systems, waste management must be considered as a priority issue. The environmental impact of coal and oil shale industry consists of issues such as contamination of the atmosphere, soil, and waterways by toxic heavy metals [7, 8]. Therefore, it is quite important to promote efficient

techniques for mine waste recycling and to produce high value-added products [9]. The synthesis of zeolites from ashes, generated by the combustion of oil shale [10] or coal, has become a promising way to valorize their residues. Zeolites are widely considered as potential adsorbent for removing heavy metals from aqueous solutions.

Numerous laboratories around the world have synthesized zeolites from fly ash used for removing heavy metals [11-14]. Shawabkeh et al. have synthesized zeolites using oil shale ash by alkaline hydrothermal treatment and used them to remove cadmium and lead [15], Visa removed heavy metal ions from aqueous solutions by new zeolite materials synthesized from fly ash [16], Bao et al. have synthesized cancrinite-type zeolite from fly ash for the removal of lead, copper, nickel, cobalt, and zinc [17], Bao et al. have synthesized Na-A zeolite from oil shale ash to be used as adsorbent for copper removal [18]. In this paper, zeolites have been synthesized from fly ash (FA) and modified oil shale ash (MOSA) under identical experimental conditions. We examined the adsorption efficiency of zeolites, synthesized from modified oil shale ash (MOSA), for removing heavy metals with respect to the adsorption efficiency of zeolites synthesized from fly ash (FA). A comparative adsorption study was conducted in order to evaluate the potential of the synthesized products for the removal of lead, zinc, and chromium. The influence factors such as pH value, adsorbent mass, and initial concentration of metal ions have been examined, and the equilibrium adsorption data were fitted to Langmuir and Freundlich adsorption isotherm models.

2. Materials and Methods

2.1. Starting Materials. Fly ash used in our study is a class F fly ash [19], and it was collected from Jorf Al Asfar thermal power plant (117 Km from Casablanca, Morocco), while oil shale was obtained from the ONYHM (National Office of Hydrocarbons and Mines) [20]. Oil shale was grinded to small sizes (<1 mm). Fly ash and oil shale underwent a heat treatment at 900°C under atmospheric conditions. Modified oil shale ash (MOSA) was prepared by nitric acid treatment of oil shale ash as described in our previous work [6]. The chemical composition of FA and MOSA was determined by X-ray fluorescence (Philips, PW 2404, Magic Pro) (Table 1).

Table 1: Chemical composition of FA and MOSA (%wt.).

Components	FA (% of mass)	MOSA (% of mass)
Na_2O	0.98	0.09
MgO	2.10	3.34
Al_2O_3	34.13	5.67
SiO_2	49.11	76.37
P_2O_5	1.48	0.07
SO_3	0.67	0.10
K_2O	1.87	0.31
CaO	3.50	8.14
TiO_2	1.23	0.75
Fe_2O_3	4.40	4.81
MnO	0.05	0.02
Trace element	0.48	0.33
Total	100	100

2.2. Zeolites Synthesis. Our synthesis method consists of introducing an alkaline fusion step prior to the refluxing treatment. It was found that this step plays an important role in the optimization of reaction conditions [21]. Larger amounts of aluminosilicates can be dissolved, and a high crystalline zeolite phase can be obtained employing this method. In a typical synthesis process, 5 g of raw material (FA or MOSA) was dry mixed with 1, 2, 4, and 8 g NaOH pellets for 30 min and the resultant mixture was fused at 650°C for 1 h. The fused product was ground in a porcelain mortar, weighed, and then was dissolved in distilled water (mass-to-liquid ratio = 1/10) under stirring conditions for 2 hours to form the amorphous precursors. Refluxing process was carried out in Pyrex one-neck round-bottom flask in a heating mantle, and temperature was maintained at 100°C. The refluxing period was fixed at 24 hours. Mineralogical and composition of the raw materials and the reaction productions were determined by powder X-ray diffraction (panalytical's X'pert pro-X-ray diffractometer with Cu Kα radiation (Kα = 1.5418 A°)), with the 2θ angle varying between 3° and 90°. Major and minor phases were performed with semiquantitative method on the basis of the intensity counts of specific reflections, the density, and the mass adsorption coefficient of the identical mineral phases [22]. FTIR characterization of FA, MOSA, and the reaction products was conducted with a VERTEX 70 spectrometer equipped with the digitec detector. The samples were prepared according to the KBr pellet method and then were scanned in a transmission mode with 4 cm^{-1} resolution at the range of 4000 to 400 cm^{-1}. The morphological characteristics of FA, MOSA, and synthetic products were observed by JEOL JMS 5500 scanning electron microscope, equipped with SUTW-Sapphire detector for EDX analysis using ZAF method for the quantification. The experimental conditions and the percentage crystallinity of the reaction products are summarized in Table 2.

2.3. Adsorption Experiments. The adsorption experiment was conducted using the reaction products ZV4 and ZM4 synthesized from FA and MOSA and mainly composed of Na-P1 and Na-P2 type zeolites, respectively. Therefore, we investigated their efficiency to adsorb lead, zinc, and chromium. In order to study the effects of pH value, contact time, adsorbent dosage, and initial concentration of metal ions, sorption tests were performed in 250 conical flasks by mixing 100 ml of metal solution of different concentrations through batch-type reactions at room temperature, with a given sorbent dose. The suspension was kept in a rotary shaker with a constant agitation speed of 200 rpm for a given time interval and pH range. Then samples were filtrated through a syringe filtration 0.22 μm, and the absorbance was measured using atomic adsorption spectroscopy (ICP AES Ultima 2). Evaluation of pH value effect on the adsorption of metal ions onto ZV4 and ZM4 was performed in the same condition as noted above with an initial metal ions concentration of 100 mg/l, adsorbent dose of 0.2 g, and

Table 2: Experimental conditions and the percentage crystallinity of the reaction products.

Starting material	Experimental conditions							Reaction product	Crystallinity (%)
	Test symbol	NaOH mass	Fusion		Agitation (h)	Refluxing			
			T (°C)	t (min)		T (°C)	t (h)		
FA (5 g)	ZV1	1	650	2	2	100	12	—	—
	ZV2	2	650	2	2	100	12	Na-P1	20.1
	ZV3	4	650	2	2	100	12	Na-P1	64.4
	ZV4	8	650	2	2	100	12	Na-P1	92.7
MOSA (5 g)	ZM1	1	650	2	2	100	12	—	—
	ZM2	2	650	2	2	100	12	Analcime	81.1
	ZM3	4	650	2	2	100	12	Na-P2	72.1
	ZM4	8	650	2	2	100	12	Na-P2	83.6

equilibrium time of 60 min. The pH value was adjusted between 2 and 8 with adding some volume of HCl 0.1 M and NaOH 0.1 M. Adsorption kinetics was studied by adding 0.2 g of adsorbent into 100 ml of metal ions solution (100 mg/l). The pH of the mixture was fixed in the range between 5 and 6 for lead and zinc while for chromium, it was fixed between 2 and 3. The adsorption capacity of metal ions (Q_e) and the removal efficiency are calculated by the following equations:

$$Q_e = \frac{(C_0 - C_e) \times V}{m},$$
$$\text{Removal efficiency } (\%) = \frac{C_e - C_0}{C_0} \times 100, \quad (1)$$

where Q_e is the adsorption capacity (mg/g), C_0 is the initial metal ion concentration in solution (mg/l), C_e is the equilibrium concentration (mg/l) after adsorption, V is the solution volume (l), and m is the mass of adsorbent (g). The Langmuir and Freundlich isotherm adsorption models were presented by their linear form, showing the variation of C_e/Q_e and Ln Q_e against, respectively, C_e and Ln C_e.

3. Results and Discussion

3.1. Characterization of Raw Materials and Synthesized Zeolites. The chemical composition of fly ash and modified oil shale ash is given in Table 1. Heat treatment of FA led to the complete reduction of organic matter, while heat and acid treatment of OSA reduced considerable amount of CaO (from 38.74% to 8.14%) [6]. Figures 1 and 2 display the X-ray diffraction patterns of the zeolite synthesis from FA and MOSA, respectively. The semiquantitative X-ray diffraction analysis of fly ash, by the reference intensity ratio method, showed that mullite constitutes more than 50% of the mineralogical composition. Hematite and magnetite do not exceed 1% of this composition while amorphous phase constitutes 27.5%. When the fly ash was activated with 1 g of NaOH, peaks of mullite and quartz decreased but no zeolite was formed; however, new peaks corresponding to sodium aluminosilicate (NaAlSiO4) have been detected. The zeolite Na-P1 appeared only when 2 g of NaOH was used. The intensity of its peaks increased with increasing the mass of NaOH. An excess of NaOH led to the total disappearance of

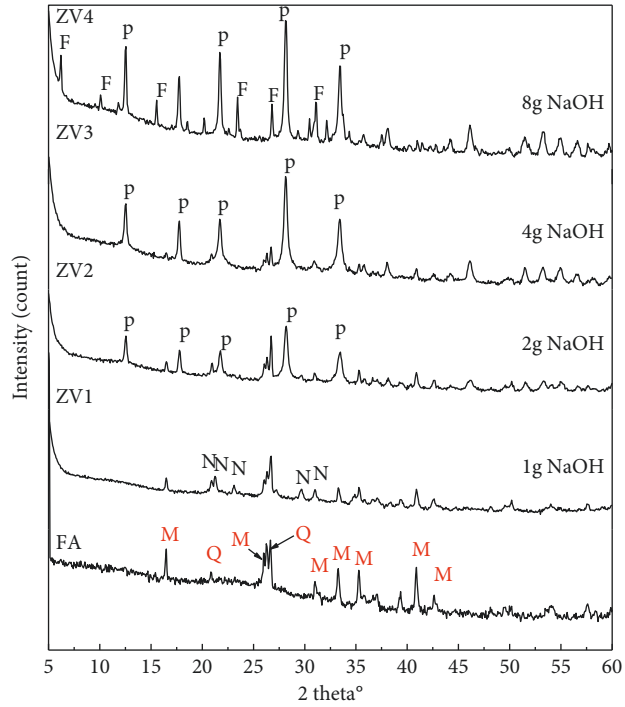

Figure 1: Patterns of FA and synthesis products. M: mullite, Q: quartz, N: sodium aluminosilicate, P: zeolite Na-P1, and F: zeolite Na-X.

mullite and quartz peaks and to the formation of Na-X faujasite type zeolite while the crystallinity of Na-P1 attained 92.7% [23]. For MOSA, we observed that the amorphous phase was the major content (50%), while augite and quartz contents were 34.3% and 15.7%, respectively. The treatment of MOSA with 1 g of NaOH resulted in complete augite dissolution while quartz was not affected. When MOSA was activated with 2 g of NaOH, analcime type zeolite was formed with a crystallinity of 81.1%. Also, a minor amount of Na-P2 type zeolite was detected. The crystallinity of Na-P2 increased with increasing the amount of NaOH while that of the analcime decreased. In the meantime, quartz disappeared completely when MOSA was treated with 4 g of NaOH. The crystallinity of Na-P2 has reached its maximum (83.6%) with 8 g of NaOH [24].

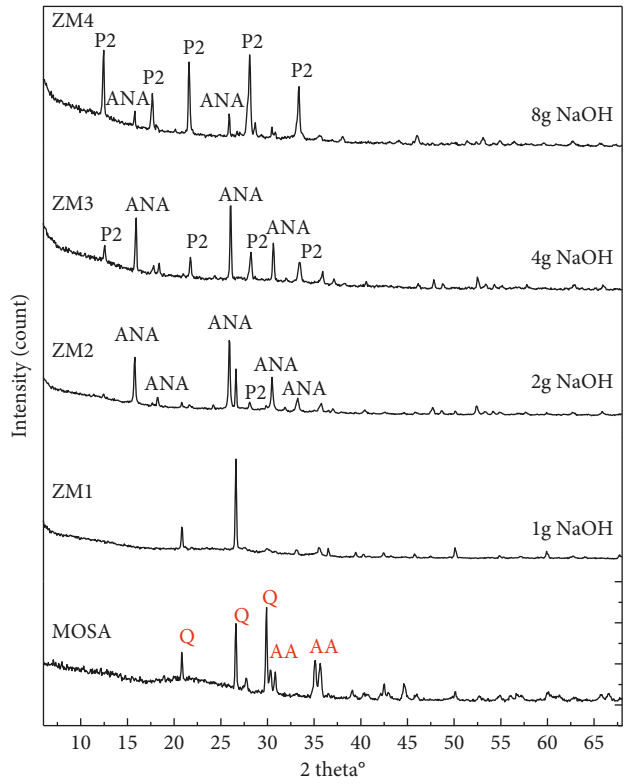

Figure 2: XRD patterns of MOSA and synthesis products. A: augite, Q: quartz, ANA: analcime, and P2: zeolite Na-P2.

Figures 3 and 4 show the FTIR spectra of the products obtained after reaction of FA and MOSA with 1 g, 2 g, 4 g, and 8 g of NaOH, respectively. The characteristic peaks of fly ash disappeared while new peaks were detected indicating the formation of new products. The bands in the region 420–500 cm^{-1} were attributed to the internal deformations of the zeolite tetrahedron δ O–(Si; Al)–O. The original band at 466 cm^{-1} shifted to lower frequencies with increasing the amount of NaOH. The bands in the region 500–650 cm^{-1} were associated with the vibrations of the double rings (4-membered ring and 6-membered ring). The intensity of the initial band at 555 cm^{-1} decreased until its total disappearance as the mass of NaOH increased. A new band was detected at 607 cm^{-1}, and its intensity increased in function of the mass of NaOH. The bands characterizing the Al^{IV}–O stretching vibrations of the mullite tetrahedron at 732 cm^{-1} and 910 cm^{-1} disappeared. A new band was formed around 747 cm^{-1}, and its intensity gradually increased. The intensity of characteristic doublet of quartz at 774 cm^{-1} and 794 cm^{-1} decreased until total disappearance, while the band at 694 cm^{-1} disappeared in the beginning, giving rise to a new band around 684 cm^{-1}, and it can be attributed to symmetric stretching of (Si; Al)–O–(Si; Al). The bands in the region 950–1200 cm^{-1} were attributed to asymmetric stretching of O–(Si; Al)–O bonds. From Figure 3, it can be seen that the original band at 1082 cm^{-1} was replaced by a new band at 994 cm^{-1}. This band moved to low frequencies before returning to its original position [25]. Figure 4 illustrates the FTIR spectra of the products obtained after the reaction of MOSA with 1 g, 2 g, 4 g, and 8 g of NaOH, respectively. The spectrum corresponding to the activation of MOSA with 1 g of NaOH shows the disappearance of the peaks associated with augite, and the peaks remaining in the spectrum were almost identical to those with characteristic peaks of quartz. The original band located at 470 cm^{-1} shifted to 440 cm^{-1}. Its intensity decreased slowly as the mass of NaOH progressed, and this band was attributed to the internal deformations of the zeolite tetrahedron δ O–(Si; Al)–O. In the range 500–650 cm^{-1}, a new band appeared at 607 cm^{-1}, and it was associated with the vibrations of the double rings (4-membered ring and 6-membered ring). The initial band at 528 cm^{-1} disappeared. In the region 650–850 cm^{-1}, new bands were detected around 690 cm^{-1} and around 750 cm^{-1} and their intensities increased with the increase of the mass of NaOH, while the band around 776 cm^{-1} decreased in intensity, and these bands were attributed to symmetric stretching of (Si; Al)–O–(Si; Al) bonds. The peaks in the 950–1200 cm^{-1} region were attributed to asymmetric stretching of O–(Si; Al)–O bonds. The initial bands at 1103 cm^{-1} and 970 cm^{-1} were replaced by a band at 994 cm^{-1}. This band first moved to high frequencies to 1030 cm^{-1} and then returned to the low frequencies [25, 26].

Figure 5(a) illustrates the SEM-determined microstructure characteristics of fly ash, and generally, the particles are distinguished by their spherical shape and smooth surface [26]. Figure 5(b) shows the synthesized product ZV4. We noticed the presence of lamellar structures identified by X-ray diffraction as zeolite Na-P1 [26]. The observation of

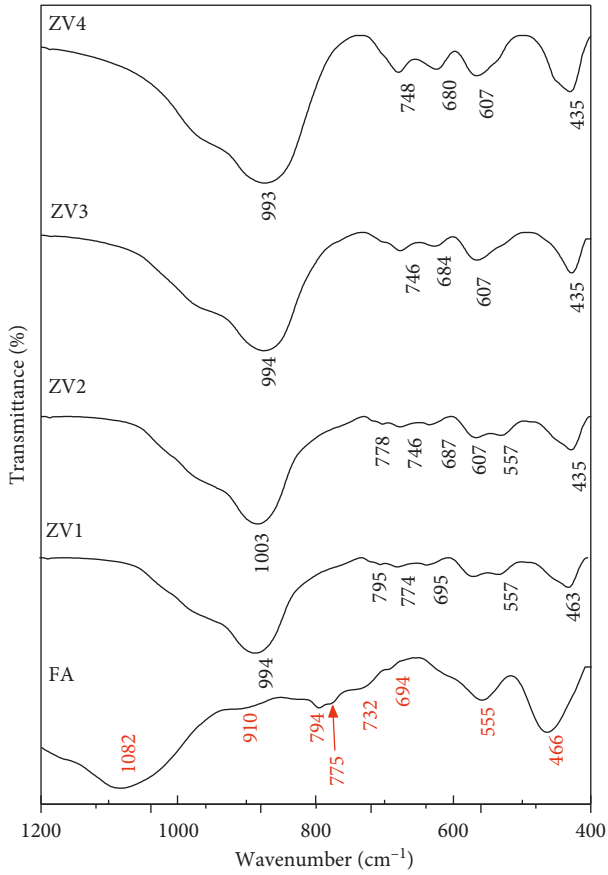

Figure 3: FTIR spectra of FA and synthesis products.

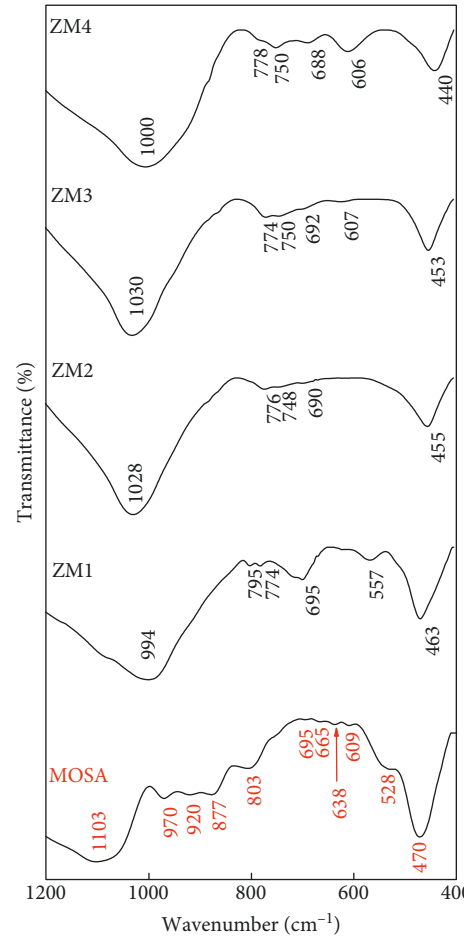

Figure 4: FTIR spectra of MOSA and synthesis products.

Figure 6(a) shows brighten whiskers (nanowires) types which were detected in different regions of the MOSA sample. They were attributed to augite, a glass-ceramic. The morphology of the synthesized product ZM4 obtained by alkaline fusion of MOSA followed by refluxing was shown in Figure 6(b). We noticed the presence of aggregates consisting of flat shapes oriented in all directions. They could be attributed to the zeolite Na-P2 [24, 27].

3.2. Sorption Experiments

3.2.1. Effect of pH. The pH value plays an important role in the adsorption process of heavy metals since it influences the surface charge of the adsorbent, the degree of ionization of the adsorbate. It can also affect the degree of dissociation of the functional groups related to the active sites of the adsorbent [28]. It has been reported that the adsorption of heavy metals was very sensitive to pH variation by controlling the potential precipitation of hydroxides and the type of speciation [29]. Figure 7 shows the influence of the pH value on the removal efficiency of heavy metals by ZV4 and ZM4. At pH = 2, the percentage of adsorption of lead and zinc on ZV4 and ZM4 did not exceed 15 % and then increased rapidly with the pH value attaining the maximum of 100% when the pH = 7. The maximum of removal efficiency of chromium was registered at pH = 2 (47. 34% for ZM4 and 43.78 % for ZV4), then the removal efficiency decreased with the pH value. The results of these experiments are in agreement with the literature [30]. The acidic proprieties of sodium zeolite Na-P are weak. Indeed, in aqueous solutions Na-P can easily release sodium and capture a proton through a cation exchange process according to the following reaction [30]:

$$\text{Z-Na} + \text{H}_2\text{O} \longleftrightarrow \text{ZH} + \text{Na}^+, \text{OH}^-. \quad (2)$$

At low pH, metal ions adsorption was difficult and this could be attributed to the competition between the excess of proton H^+ and the ion metal on the surface of the adsorbent. Therefore, increasing the pH value led the augmentation of the removal efficiency of Pb(II) and Zn(II) by ZV4 and ZM4. However, we cannot emphasize the role of our synthesized products in the removal of lead and zinc for pH > 7 because above this value, the effect of adsorption was deregulated by the phenomenon of precipitation of lead (Pb(OH), Pb $(OH)_2$) and zinc (Zn (OH), Zn $(OH)_2$) [29]. For chromium, it can be seen from the results shown in Figure 7 that its removal efficiency reached the maximum when the pH = 2, and then the yield decreased progressively with pH. Considering that in acidic solution, hexavalent chromium exists in the anionic form ($Cr_2O_7^{2-}$, $HCrO_4^-$, $Cr_3O_{10}^{2-}$, and $Cr_4O_{13}^{2-}$) and that the sites of the synthesized products become protonated adsorption and then was favored [31]. At

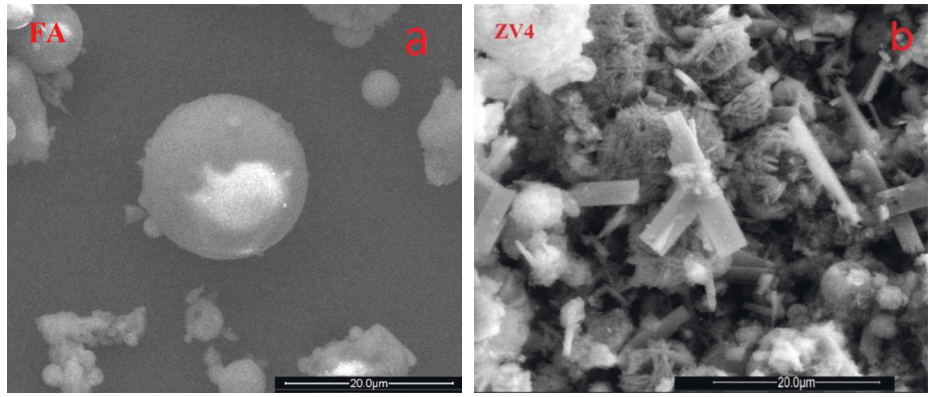

Figure 5: SEM images of fly ash and the synthesis product ZV4 morphology.

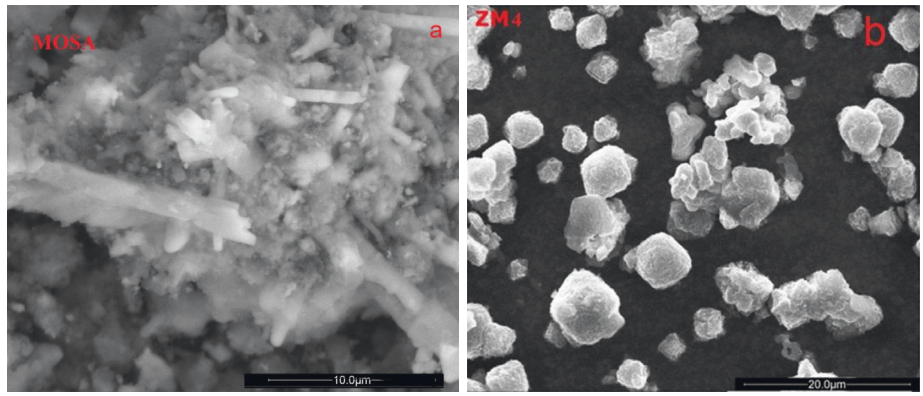

Figure 6: SEM images of MOSA and the synthesis product ZM4 morphology.

high pH, there was a competition between OH^- and the $Cr_2O_7^{2-}$ form, the protonation of the active sites of the adsorbents was weakened, and the adsorption was difficult [32].

3.2.2. Effect of Contact Time. Figure 8 shows that the removal efficiency of heavy metals varies with stirring time, and the removal efficiency of lead, zinc, and chromium reached the maximum after 45 min for ZM4 as well as for ZV4. Then metal concentration remained almost constant for the rest of the time intervals. On the contrary, the removal efficiency of chromium decreased gradually, which can be explained by the desorption phenomena. Based on the experimental results, we can conclude that lead has an affinity for ZM4 greater than that for ZV4 with a maximum removal efficiency of 79.77% and 69.97%, respectively, while zinc has a remarkable affinity for ZV4 (85.7%) superior than this for ZM4 (79.29 %). In the end, chromium has only a limited affinity for the two adsorbents (46.56% and 44.13%, respectively, for ZM4 and for ZV4), despite the favorable conditions of the acidic pH. This result can be attributed to other factors that influence the adsorption phenomena such as polarity, polarizability, and adsorbed ion size [26].

3.2.3. Effect of Adsorbent Dosage. The effect of the adsorbent dosage on the removal of heavy metals was conducted with mixing a mass of adsorbent ranging from 0.05 g to 0.4 g into 100 ml of each metal solution (C0 = 100 mg/l)). As it can be seen from Figure 9, the percent removal of lead and zinc increased with increasing the mass of adsorbent. The total removal of zinc was reached with 0.3 g of both adsorbents (ZM4 and ZV4) while for the removal of lead, it was reached with 0.3 g of ZM4 and 0.4 g of ZV4. In fact, with increase of the adsorbent mass, negatively charged exchange sites became more numerous, and consequently, the probability of adsorption increased [26]. For chromium, we observed that its removal efficiency increased rapidly in the first stage and then progressed slowly. A mass of 0.7 g of ZM4 and ZV4 removed only 78.43% and 67.23% of chromium, respectively.

3.2.4. Effect of Initial Metal Concentration. Figure 10 depicts the effect of initial concentration on the removal of heavy metals at various concentrations from 25 to 400 mg/l with 0.3 g and 0.7 g mass of both adsorbents, respectively, for the adsorption of zinc and the adsorption of chromium while for the adsorption of lead, the mass of ZM4 and ZV4 was fixed at 0.3 g and 0.4 g, respectively. As we can observe from the same figure, when the initial concentration of lead and zinc increased from 25 to 100 mg/l, the adsorption capacity of ZV4 increased, respectively, from 6.25 to 24.28 mg/g for lead and from 8.33 to 33.02 mg/g for zinc while the adsorption

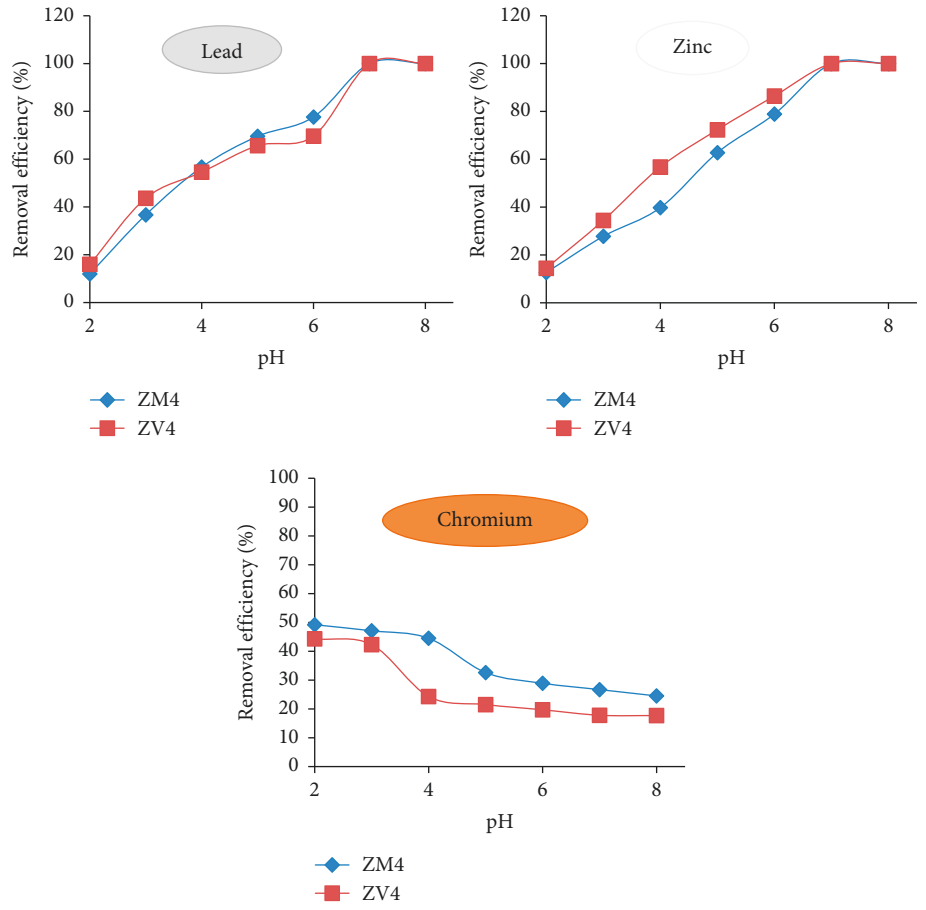

Figure 7: Effect of pH on the removal of heavy metals by ZV4 and ZM4.

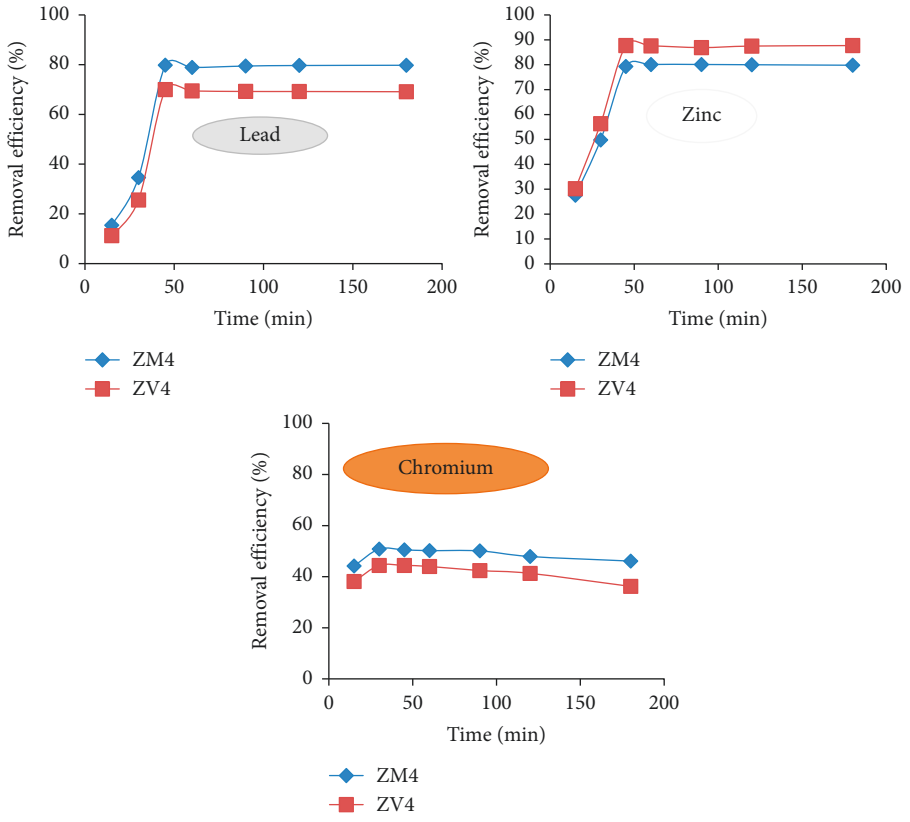

Figure 8: Effect of contact time on the removal of heavy metals by ZV4 and ZM4.

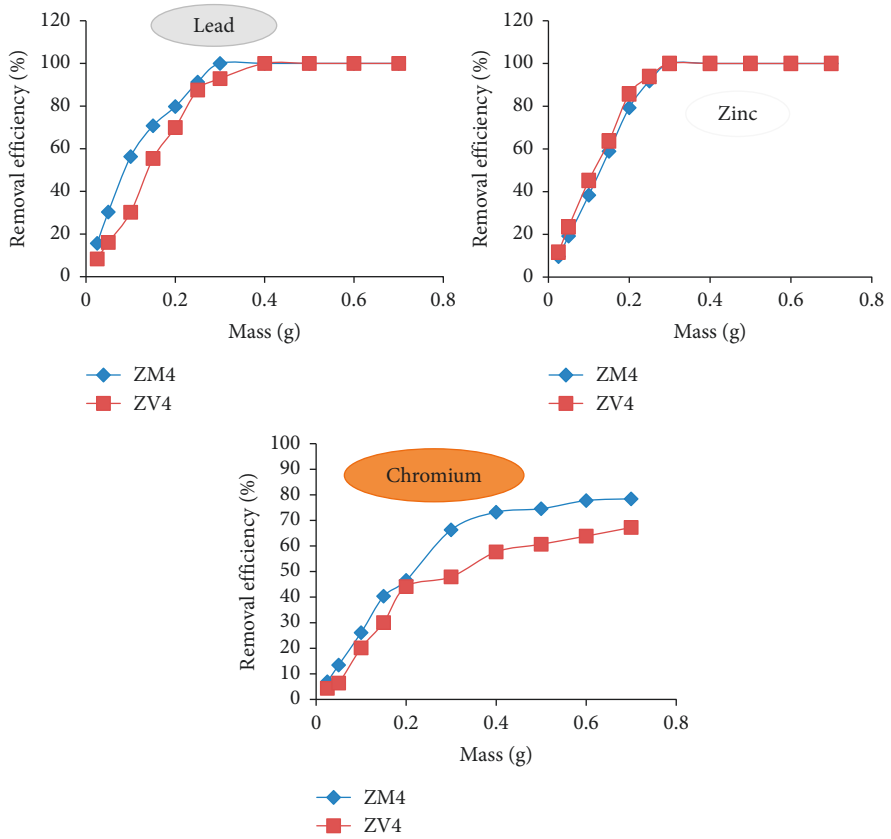

Figure 9: Effect of mass adsorbent on the removal of heavy metals by ZV4 and ZM4.

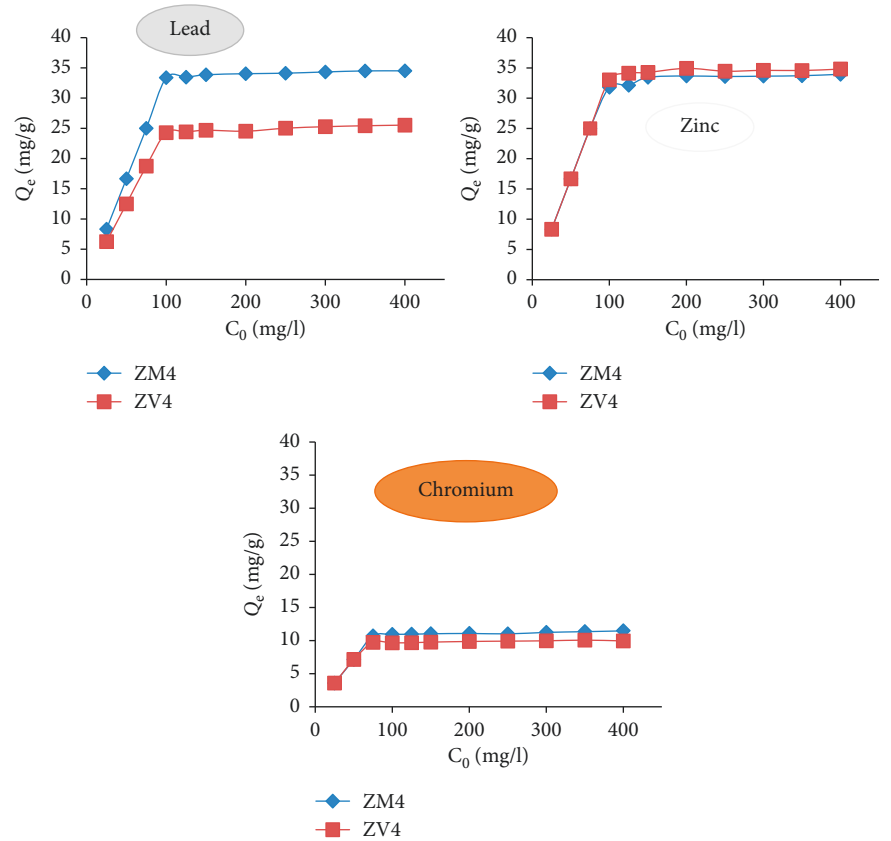

Figure 10: Effect of initial metal concentration on the adsorption of heavy metals onto ZV4 and ZM4.

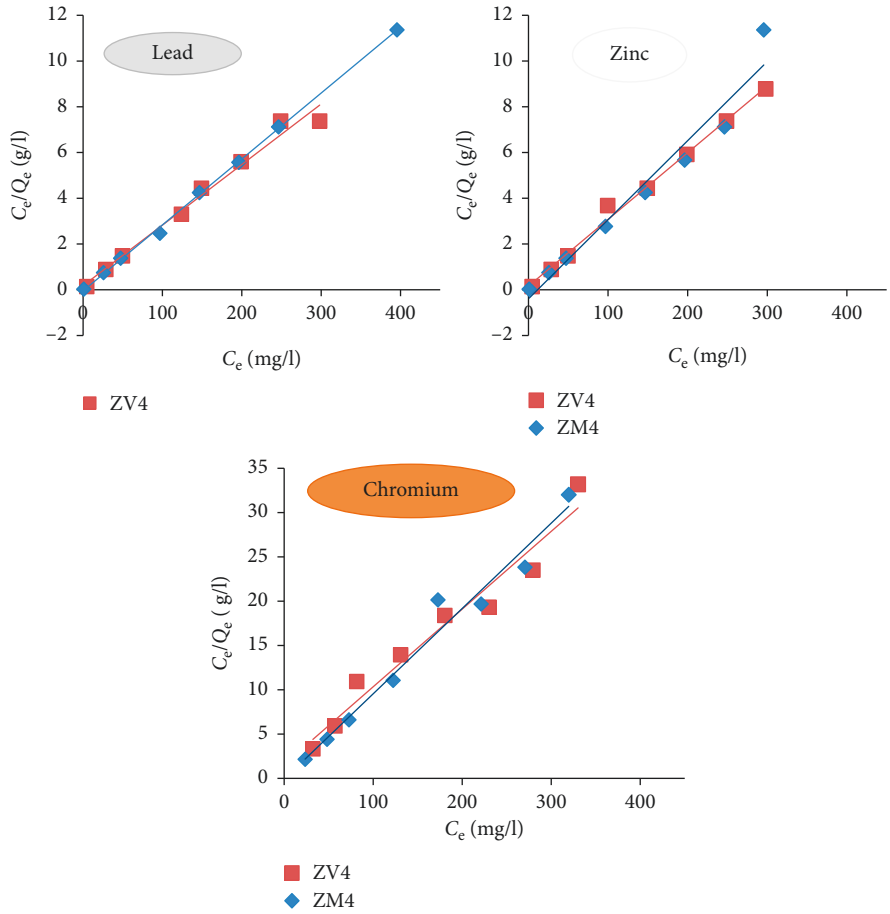

Figure 11: Langmuir isotherm representing variation of adsorption C_e/Q_e with respect to C_e for adsorption of heavy metals onto ZV4 and ZM4.

capacity of ZM4 increased from 8.33 to 33.38 mg/g for lead and from 8.33 to 31.81 mg/g for zinc. The adsorption capacity of ZM4 and ZV4 for chromium started with a value of 3.57 mg/g and attained values of 10.93 mg/g and 9.67 mg/g, respectively, when the initial concentration of chromium increased from 25 mg/l to 75 mg/l. However, the adsorption capacity of ZV4 and ZM4 remained nearly constants when the initial concentration of lead and zinc was higher than 100 mg/l due to the saturation of all active sites on the pore surface of the adsorbents [33]. Nevertheless, the stagnation of the adsorption capacity of ZM4 and ZV4 when the initial concentration of chromium exceeded the value of 75 mg/l can be explained by the fact that the maximum adsorption capacity was reached under the effect of other factors that influenced the adsorption phenomena such as charge, size, and polarizability of the metal ion [28].

3.2.5. Adsorption Isotherm. The adsorption process can be described using an adsorption isotherm. The curve of this isotherm is presented by a mathematical equation. We have retained the linear model of Langmuir [34] and the linear model of Freundlich [35]. These models are the most commonly used. For the Langmuir model, it is assumed that the adsorbent has a limited adsorption capacity (Q_m), that all the active sites are identical, that each site can complex only one solute molecule alone (monolayer adsorption), and that there are no interactions between the adsorbed molecules. However, Freundlich isotherm is an empirical model which can be applied to the adsorption onto heterogeneous surfaces. The Langmuir isotherm and the Freundlich isotherm models are presented by the following equations:

$$\frac{C_e}{Q_e} = \frac{C_e}{Q_m} + \frac{1}{b \times Q_m}, \tag{3}$$

$$\text{Ln } Q_e = \text{Ln } K_f + nf \text{ Ln } C, \tag{4}$$

where Q_m is the maximum adsorption capacity (mg/g), Q_e is the quantity adsorbed at equilibrium (mg/g), C_e is the concentration of adsorbate in solution at equilibrium (mg/l), and b is the equilibrium constant of Langmuir (l/mg). nf and K_f (mg/g (l/mg)^n) are both the Freundlich constants providing an indication of the adsorption intensity and capacity, respectively. If $nf > 1$, the adsorption is unfavorable; if $nf = 1$, the adsorption is linear; and if $nf < 1$, the physical adsorption is favorable. Langmuir and Freundlich adsorption isotherm and their parameters are presented in

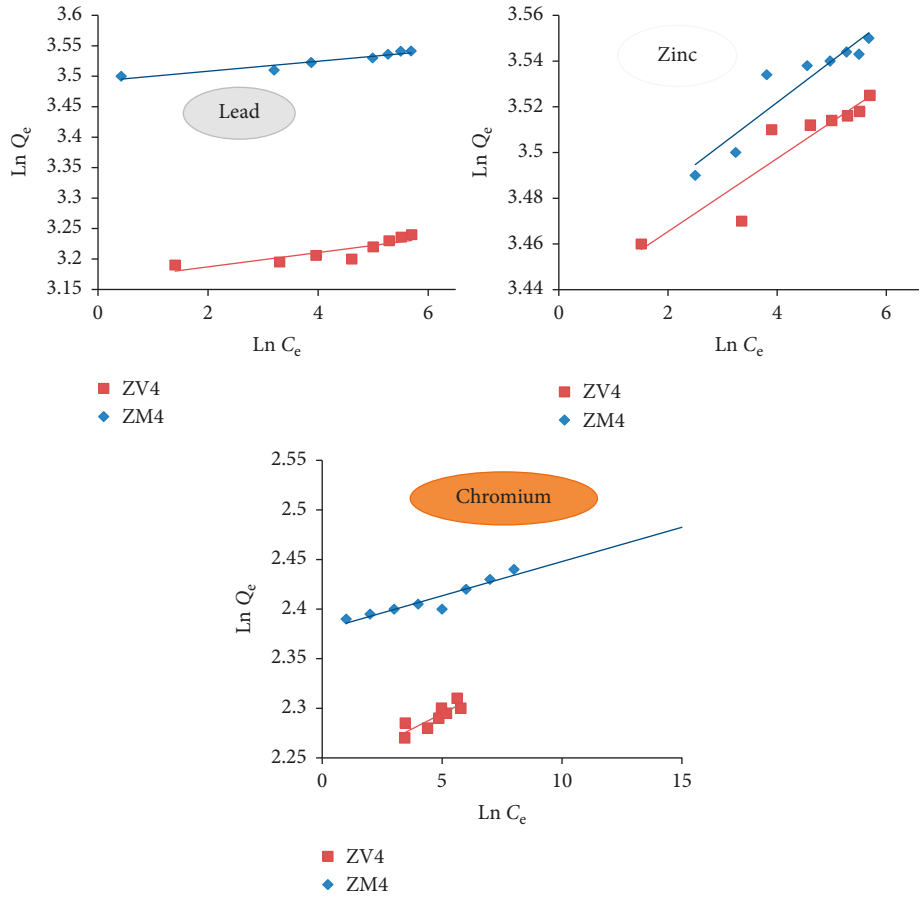

Figure 12: Freundlich isotherm showing the variation of $\ln(Q_e)$ against the $\ln(C_e)$ for adsorption of heavy metals onto ZV4 and ZM4.

Table 3: Langmuir and Freundlich isotherm parameters for the adsorption of lead, zinc, and chromium onto ZV4 and ZM4.

Metal ions	Langmuir model			Freundlich model		
	Q_m (mg/g)	b (l/mg)	R^2	K_f (mg/g)	nf	R^2
ZV4						
Lead	25.64	0.48	0.990	23.57	0.01	0.751
Zinc	34.24	0.58	0.993	30.87	0.02	0.867
Chromium	10.41	0.8	0.957	9.29	0.01	0.745
ZM_4						
Lead	34.96	0.4	0.991	32.78	0.008	0.918
Zinc	29.41	0.87	0.957	31.50	0.02	0.880
Chromium	11.49	0.05	0.971	10.69	0.006	0.889

Figure 11, Figure 12, and Table 3. The results showed that lead has better adsorbability for ZM4 compared to ZV4 with maximum capacities of 34.96 mg/g and 25.64 mg/g, respectively. While ZV4 had an adsorption capacity for zinc superior to that of ZM4, their maximum adsorption capacities are 34.24 mg/g and 29.41 mg/g, respectively. Chromium showed a reduced adsorbability. The maximum adsorption capacity values were 10.41 mg/g and 11.49 mg/g, respectively, for ZM4 and for ZV4. According to the Freundlich model, the values of nf indicate that the adsorption of lead, zinc, and chromium onto both adsorbents was favorable. Based on the coefficients of correlation (R^2) shown in Table 3, the adsorption isotherms can be best described by the Langmuir model.

4. Conclusion

This work investigates the possibility of fly ash (FA) and modified oil shale ash (MOSA) as starting materials for zeolites synthesis under identical experimental conditions. Characterization of synthesis products was made by several analytical techniques. The products ZV4 and ZM4, produced from the conversion of FA and MOSA and composed mainly of Na-P1 and Na-P2 type zeolites, respectively, were selected for the adsorption tests. The crystallinity of Na-P1 and Na-P2 was found to be 92.7% and 83.6%, respectively. A comparative adsorption study was conducted in order to evaluate the potential of these reaction products for heavy metals adsorptions. The results of the removal experiments suggest that ZV4 and ZM4 can be considered as efficient and low-cost adsorbents. The affinity of ZV4 for the removal of heavy metal adsorption was in decreasing order Zn > Pb > Cr while the ZM4 affinity is reported to follow the decreasing order Pb > Zn > Cr. The maximum adsorption capacities for Pb, Zn, and Cr estimated from Langmuir adsorption isotherms were found to be 25.64, 34.24, and 10.41 mg/g and 34.96, 29.41, and 11.49 mg/g for ZV4 and ZM4, respectively.

From these results, the following conclusion can be drawn: zeolites synthesized from MOSA may be considered as effective as those synthesized from FA for heavy metals adsorption.

Data Availability

The data that support the findings of this study are available on request from the corresponding author.

Conflicts of Interest

The authors declare that they have no conflicts of interest regarding the publication of this paper.

Acknowledgments

Analytical instrument facilities were provided by the UATRS-CNRST (Unité d'Appui à la Recherche Scientifique-Centre National de la Recherche Scientifique et Technique), Rabat, Morocco. The authors would like to thank the technicians and the engineers of UATRS.

References

[1] S. Yaday, V. Srivastava, S. Banerjee, F. Gode, and Y. C. Sharma, "Studies on the removal of nickel from aqueous solutions using modified riverbed sand," *Environmental Science and Pollution Research*, vol. 20, no. 3, pp. 558–567, 2013.

[2] F. Fu and Q. Wang, "Removal of heavy metal ions from wastewaters: a review," *Journal of Environmental Management*, vol. 92, no. 3, pp. 407–418, 2011.

[3] M. Nascimento, P. S. M. Soares, and V. P. D. Souz, "Adsorption of heavy metal cations using coal fly ash modified by hydrothermal method," *Fuel*, vol. 88, no. 9, pp. 1714–1719, 2009.

[4] Y. N. Mata, M. L. Blázquez, A. Ballester, F. Gonzjlez, and J. A. Munoz, "Sugar-beet pulp pectin gels as biosorbent for heavy metals: preparation and determination of biosorption and desorption characteristics," *Chemical Engineering Journal*, vol. 150, no. 2-3, pp. 289–301, 2009.

[5] S. Babel and T. A. Kurniawan, "Low-cost adsorbents for heavy metals uptake from contaminated water: a review," *Journal of Hazardous Material*, vol. B97, no. 1–3, pp. 219–243, 2003.

[6] https://www.globalsyngas.org/uploads/downloads/GTC_Waste_to_Energy.pdf.

[7] https://energy.gov/fe/services/petroleum-reserves/naval-petroleum-reserves/oil-shale-and-other-unconventional-fuels.

[8] C. Heidrich, H. G. Feuerborn, and A. Weir, "Coal combustion products: a global perspective," in *Proceedings of World of Coal Ash Conference*, Lexington, KY, USA, April 2013.

[9] C. Ellyett and A. Fleming, "Thermal infrared imagery of the burning mountain coal fire," *Remote Sensing Environment*, vol. 3, no. 1, pp. 79–86, 1974.

[10] K. Nabih, "Caractérisation et traitements thermiques des schistes bitumeux des sous couches R de Tarfaya sous différentes atmosphères (N2, He, air et vapeur d'eau), Utilisation du Ciment dans la production du ciment," D Etat thesis, University of Mohamed V, Rabat, Morocco, 1997.

[11] A. Hamadi and K. Nabih, "Alkali activation of oil shale ash based ceramics," *E-Journal of Chemistry*, vol. 9, no. 3, pp. 1373–1388, 2012.

[12] H. Bergk, M. Porsch, and J. Drews, "Conversion of solid primary and recycled raw materials to zeolite-containing products. Part VI: continuous manufacture of zeolite A containing products," *Chemische Technik*, vol. 39, pp. 308–310, 1987.

[13] H. Höller and U. Barth-Wirsching, "Zeolite formation from fly ash," *Fortschritte Der Mineralogie*, vol. 63, pp. 21–43, 1985.

[14] F. Mondragón, F. Rincón, L. Sierra, J. Escobar, J. Ramírez, and J. Fernández, "New perspectives for coal ash utilization: synthesis of zeolitic materials," *Fuel*, vol. 69, no. 2, pp. 263–266, 1990.

[15] R. Shawabkeh, A. Al-Harahsheh, M. Hami, and A. Khlaifat, "Conversion of oil shale ash into zeolite for cadmium and lead removal from wastewater," *Fuel*, vol. 83, no. 7-8, pp. 981–985, 2004.

[16] M. Visa, "Synthesis and charcterisation of new zeolite materials obtained from fly ash for heavy metals removal in advanced waste water treatment," *Powder Technology*, vol. 294, pp. 338–347, 2016.

[17] W. Bao, H. Zou, S. Gan, X. Xu, G. Ji, and K. Zheng, "Adsorption of heavy metal ions from aqueous solutions by zeolite based on oil shale ash: kinetic and equilibrium studies," *Chemical Research in Chinese Universities*, vol. 29, no. 1, pp. 126–131, 2013.

[18] W. Bao, L. Liu, H. Zou et al., "Removal of Cu^{2+} from aqueous solutions using Na-a zeolite from oil shale ash," *Chinese Journal of Chemical Engineering*, vol. 21, no. 9, pp. 974–982.

[19] *Standard Specification for Coal Fly Ash and Raw or Calcined Natural Pozzolan for Use in Concrete, Active Standard ASTM C618, Book of Standards*, Vol. 04, ASTM, West Conshohocken, PA, USA, 2003.

[20] "Office nationale des hydrocarbures et des mines (ONYHM)," http://www.onhym.com/.

[21] G. Gottardi and E. Galli, *Naural Zeolites*, Springer-Verlag, Berlin, New York, NY, USA, 1985.

[22] R. L. Snyder and D. l. Bish, "Quantitative analysis," in *Modern Powder Diffraction Reviews in Mineralogy*, D. L. Bish and J. E. Post, Eds., vol. 20, pp. 101–144, Mineralogical Society of America, Washington, DC, USA, 1989.

[23] S. Rayalu, S. U. Meshram, and M. Z. Hasan, "Highly crystalline faujasitic zeolites from fly ash," *Journal of Hazardous Materials*, vol. 77, no. 1–3, pp. 123–131, 2000.

[24] T. S. Hua, *Sorption Behavior of Zeolite P and its Modified forms in the Removal of Selected Hazardous Metals and Oxyanions from Aqueous media*, Universiti Teknologi Malaysia, Johor Bahru, Malaysia, 2007.

[25] E. M. Flaningen, H. A. Khatami, and H. A. Szymanski, *Molecular Sieve Zeolites-I*, Vol. 16, ACS Publications, Washington, DC, USA, 1971.

[26] C. Rios, *Synthesis of Zeolites from Geological Materials and Industrial Wastes for Potential Application in Environmental Problems*, University of Wolverhampton, England, Wolverhampton, UK, 2008.

[27] L. V. C. Rees and S. Chandrasekhar, "Hydrothermal reaction of kaolinite in presence of fluoride ions at pH^{pH}less than 10," *Zeolites*, vol. 13, no. 7, pp. 534–541, 1993.

[28] P. X. Sheng, Y.-P. Ting, J. P. Chen, and L. Hong, "Sorption of lead, copper, cadmium, zinc, and nickel by marine algal biomass: characterization of biosorptive capacity and investigation of mechanisms," *Journal of Colloid and Interface Science*, vol. 275, no. 1, pp. 131–141, 2004.

[29] R. PeñaPenilla, A. Guerrero Bustos, and S. Goñi Elizalde, "Immobilization of Cs, Cd, Pb and Cr by synthetic zeolites

from Spanish low-calcium coal fly ash," *Fuel*, vol. 85, no. 5-6, pp. 823–832, 2006.

[30] S. Khemaissia, "Synthesis and characterization of zeolite mate- rials. Application in radioactive waste treatment," Ph.D. thesis, University of Science and Technology (USTHB), Algiers, Algeria, 2008.

[31] R. Leyva-Ramos, A. Juarez-Martinez, and R. M. Guerrero-Coronado, "Adsorption of chromium (VI) from aqueous solutions on activated carbon," *Water Science Technology*, vol. 30, no. 9, pp. 191–197, 1994.

[32] R. Leyva-Ramos, A. Jacobo-Azuara, P. E. Diaz-Flores, R. M. Guerrero-Coronado, J. Mendoza-Barron, and M. S Berber-Mendoza, "Adsorption of chromium (VI) from water solution onto oragnobentonite," *Environmental Engineering and Management Journal*, vol. 18, no. 5, pp. 311–317, 2008.

[33] R. Shawabkeh, "Equilibrium study and kinetics of Cu2+ removal from water by zeolite prepared from oil shale ash," *Process Safety and Environmental Protection*, vol. 87, no. 4, pp. 261–266, 2009.

[34] I. Langmuir, "The constitution and fundamental properties of solids and liquids," *Journal of the American Chemical Society*, vol. 40, no. 9, pp. 1361–1403, 1918.

[35] H. Freundlich, *Colloid and Capillary Chemistry*, Methuen, London, UK, 1926.